

AN APPROXIMATE ANALYTICAL SOLUTION TO THE DIFFUSION EQUATION FOR SHORT-RANGE DISPERSION FROM A CONTINUOUS GROUND-LEVEL SOURCE

J. D. WILSON*

Atmospheric Environment Service, 4905 Dufferin Street, Downsview, Ontario, Canada

(Received in final form 22 January, 1982)

Abstract. An easily-evaluated expression for the dimensionless concentration profile $\chi(z/z_0, x/z_0, z_0/L) = cu_*/kQ$ (or z_0cu_*/kQ) downwind of a continuous ground-level area (or line) source in the stable surface layer is obtained by integrating the diffusion equation using the Shwetz approximation method (c = concentration, Q = source strength, k = von Kármán's constant). The analytical solution compares closely with concentration profiles obtained using a trajectory-simulation model over a useful range of heights, the important discrepancies occurring at the upper edge of the plume. The analytical solution is used to generate predictions of ground-level concentration for the Project Prairie Grass experiments; good agreement with the observations is obtained at all downwind distances (50 to 800 m).

1. Introduction

This paper is concerned with short-range dispersion of a passive admixture from a continuous ground-level source in the horizontally homogeneous neutrally or stably stratified atmospheric surface layer. An approximate analytical solution to the diffusion equation (derived below) is obtained and shown to be in good agreement both with solutions obtained using a trajectory-simulation (Lagrangian) model and with experimental data. The analytical solution is composed of elementary functions and is easily evaluated.

Let u , c , and F be respectively the time-averaged windspeed in the horizontal (x) direction, the admixture concentration, and the turbulent flux density along the vertical (z) direction. Assuming the motion to be two-dimensional and neglecting the divergence in the horizontal of the horizontal turbulent flux density, conservation of the mass of admixture may be expressed by

$$u \frac{\partial c}{\partial x} = - \frac{\partial F}{\partial z}. \quad (1)$$

Under the restriction that at all points the mean concentration gradient $\partial c/\partial z$ does not change significantly over a distance of the order of the local turbulent length scale, one may relate the vertical flux to the mean concentration gradient by

$$F = -K \frac{\partial c}{\partial z} \quad (2)$$

* Present Affiliation: New Zealand Meteorological Service, P.O. Box 722, Wellington, New Zealand.

where K is the eddy diffusivity for the admixture. For a ground-level line source, one expects the largest values of $\partial^2 c / \partial z^2$ at very short downwind distances near the ground, where the turbulent length scale is very small. For a ground-level plane source, $\partial^2 c / \partial z^2$ will be largest near the leading edge, again close to ground. Therefore in either case it is reasonable to expect the flux-mean gradient closure scheme (K -theory) to be valid. Equation (1) becomes

$$u \frac{\partial c}{\partial x} = \frac{\partial}{\partial z} \left(K \frac{\partial c}{\partial z} \right). \quad (3)$$

The wind profile in the atmospheric surface layer is described by

$$\frac{kz}{u_*} \frac{du}{dz} = \phi_m \left(\frac{z}{L} \right)$$

where $L = -u_*^3 / (k \cdot g / T_0 \cdot H / \rho c_p)$, ϕ_m is the Monin-Obukhov universal function for momentum, u_* is the friction velocity, k is von Karman's constant (0.4 used herein), g the acceleration due to gravity, T_0 a reference temperature, H the sensible heat flux density (negative in stable stratification), ρ the density of the air, and c_p the specific heat at constant pressure. In stable stratification $\phi_m = 1 + \beta_u z / L$ with $\beta_u \approx 5$ (Dyer, 1974). Therefore

$$u(z) = \frac{u_*}{k} \left[\ln \frac{z}{z_0} + \beta_u \frac{z - z_0}{L} \right] \quad (4)$$

where z_0 is the roughness length. The logarithmic neutral wind profile follows by writing $L = \infty$.

The admixture diffusivity will be assumed to have the form

$$K = azbu_* \left/ \left(1 + \beta_K \frac{z}{L} \right) \right. \quad (5)$$

where $az = \Lambda_L^N$, the Lagrangian length scale of the turbulence in neutral stratification, and $b = \sigma_w / u_* \approx 1.25$, where σ_w is the root-mean-square vertical velocity. Wilson *et al.* (1981c) deduced that $a \approx 0.5$ by comparing predictions of a Lagrangian trajectory-simulation model of dispersion with atmospheric measurements. One may estimate $\beta_K \approx 5$ given the findings of Webb (1970) for the relationship between vapour fluxes and vapour-pressure gradients. Note that the eddy viscosity by definition obeys $K_m = ku_* z / \phi_m$. With $k = 0.4$ it follows that $\alpha = K / K_m \approx 1.6$.

In neutral stratification, Equation (3) becomes

$$\left(\frac{u_*}{k} \ln \frac{z}{z_0} \right) \frac{\partial c}{\partial x} = abu_* \frac{\partial}{\partial z} \left(z \frac{\partial c}{\partial z} \right).$$

To date no exact analytical solution to this equation has been obtained. Numerical solutions have been given by Yamamoto and Shimanuki (1961), using $K = K_m$ and by

Nieuwstadt and van Ulden (1978), using $K = K_H$ (the eddy-diffusivity for heat) and $K = 1.35 K_m$ [†]. Lebedeff and Hameed (1976) gave an approximate analytical solution for ground-level concentration, again with $K = K_m$. Several authors have obtained analytical solutions by replacing the logarithmic wind profile with a power-law profile (for example, Philip, 1959; van Ulden, 1978).

Sections 2 and 3 will describe an approximate analytical solution to Equation (3) with wind and diffusivity profiles (4) and (5) and 'flux' (i.e., specified rate of emission) boundary conditions appropriate to ground-level area and line sources. In Section 4 it will be shown that the analytical solutions are in close agreement with the predictions of a trajectory-simulation (Lagrangian) model of turbulent dispersion, and in Section 5 the analytical solutions will be compared with experimental data.

2. Solution of Diffusion Equation for a Ground-level Area Source

The first step in the solution is a transformation of Equation (3). Define $\lambda = \ln(z/z_0)$, $\xi = x/z_0$, $\Omega = z_0/L$, $N = abk$, and $\chi(\xi, \lambda) = cu_*/kQ$, where Q is the source strength [$\text{cm}^{-2} \text{s}^{-1}$]. Note that $\partial/\partial z = (1/z) \partial/\partial \lambda$. Then Equation (3) becomes

$$e^\lambda [\lambda + \beta_u \Omega (e^\lambda - 1)] \frac{\partial \chi}{\partial \xi} = N \frac{\partial}{\partial \lambda} \left[\frac{1}{1 + \beta_K \Omega e^\lambda} \frac{\partial \chi}{\partial \lambda} \right]. \quad (6)$$

Symbolising Equation (6) by $f(\dot{\chi}) = g(\chi)$, where the dot denotes differentiation with respect to ξ , an approximate solution is sought by writing

$$\chi = \chi_0 + \chi_1 + \dots$$

where

$$g(\chi_0) = 0, \quad g(\chi_1) = f(\dot{\chi}_0), \quad g(\chi_2) = f(\dot{\chi}_1), \dots$$

This approximation method was first suggested by Shwetz (1949) and was briefly summarised by Panchev *et al.* (1971). Only the first two terms will be retained in this analysis.

Define $z_\delta(\xi)$ to be the upper edge of the plume of emitted material, and let $\delta(\xi) = \ln(z_\delta/z_0)$. The chosen boundary conditions are

$$\chi_0(\xi, \delta) = \chi_1(\xi, \delta) = 0 \quad (7)$$

$$\left(\frac{\partial \chi_0}{\partial \lambda} \right)_{\lambda=0} = \frac{-r(1 + \beta_K \Omega)}{N}, \quad (8a)$$

$$\left(\frac{\partial \chi_1}{\partial \lambda} \right)_{\lambda=0} = \frac{-(1-r)(1 + \beta_K \Omega)}{N} \quad (8b)$$

[†] With von Karman's constant set at 0.35.

$$\left(\frac{\partial \chi}{\partial \lambda}\right)_{\lambda=\delta} = \left(\frac{\partial \chi_0}{\partial \lambda}\right)_{\lambda=\delta} + \left(\frac{\partial \chi_1}{\partial \lambda}\right)_{\lambda=\delta} = 0 \quad (9)$$

$$\delta(0) = 0 \quad (10)$$

$$\int_0^{\delta} \chi(\xi, \lambda) [\lambda + \beta_u \Omega (e^\lambda - 1)] e^\lambda d\lambda = \xi. \quad (11)$$

Boundary conditions (8) are derived from the expression

$$-\left(K \frac{\partial c}{\partial z}\right)_{z=z_0} = Q$$

by assuming Q may be partitioned into a contribution rQ to χ_0 , with remainder $(1-r)Q$ to χ_1 . The partitioning factor r is independent of ξ , and will be discussed later. Boundary condition (11) expresses the fact that at x the integral of the horizontal flux density up to the plume depth must have value Qx , equal to the total rate of emission upstream.

From

$$N \frac{\partial}{\partial \lambda} \left[\frac{1}{1 + \beta_K \Omega e^\lambda} \frac{\partial \chi_0}{\partial \lambda} \right] = 0$$

and boundary condition (8a) it follows that

$$\frac{\partial \chi_0}{\partial \lambda} = \frac{-r}{N} (1 + \beta_K \Omega e^\lambda). \quad (12)$$

Integration and application of boundary condition (7) gives

$$\chi_0 = \frac{r}{N} [\beta_K \Omega (e^\delta - e^\lambda) + (\delta - \lambda)]. \quad (13)$$

Differentiating, one obtains

$$\frac{\partial \chi_0}{\partial \xi} = \frac{\partial \chi_0}{\partial \delta} \frac{\partial \delta}{\partial \xi} = \frac{r \dot{\delta}}{N} (1 + \beta_K \Omega e^\delta). \quad (14)$$

Substituting (14) into the expression $g(\chi_1) = f(\chi_0)$ and integrating:

$$\frac{N^2}{\dot{\delta} r (1 + \beta_K \Omega e^\delta)} \frac{1}{1 + \beta_K \Omega e^\lambda} \frac{\partial \chi_1}{\partial \lambda} = e^\lambda (\lambda - 1 - \beta_u \Omega) + \frac{\beta_u \Omega}{2} e^{2\lambda} + \alpha_1. \quad (15)$$

Application of boundary condition (8b) gives

$$\alpha_1 = 1 + \frac{\beta_u \Omega}{2} - \frac{N(1-r)}{\delta r(1 + \beta_K \Omega e^\delta)}. \quad (16)$$

Integration of (15) gives

$$\begin{aligned} \frac{N^2}{\delta r(1 + \beta_K \Omega e^\delta)} \chi_1 = & \frac{\beta_u \beta_K \Omega^2}{6} e^{3\lambda} + \\ & + \left(\frac{\beta_u \Omega}{4} - \frac{3\beta_K \Omega}{4} - \frac{\beta_u \beta_K \Omega^2}{2} \right) e^{2\lambda} + \frac{\beta_K \Omega}{2} \lambda e^{2\lambda} + \\ & + \lambda e^\lambda + (\alpha_1 \beta_K \Omega - 2 - \beta_u \Omega) e^\lambda + \alpha_1 \lambda + \alpha_2. \end{aligned} \quad (17)$$

Using boundary condition (7),

$$\begin{aligned} \alpha_2 = & -\alpha_1 \delta - \frac{\beta_u \beta_K \Omega^2}{6} e^{3\delta} - \\ & - \left(\frac{\beta_u \Omega}{4} - \frac{3\beta_K \Omega}{4} - \frac{\beta_u \beta_K \Omega^2}{2} \right) e^{2\delta} - \\ & - \frac{\beta_K \Omega}{2} \delta e^{2\delta} - \delta e^\delta - (\alpha_1 \beta_K \Omega - 2 - \beta_u \Omega) e^\delta. \end{aligned} \quad (18)$$

Although combinations of Equations 13, 16, 17, 18 gives the solution for $\chi(\xi, \lambda)$, the function $\delta(\xi)$ has not been determined. Substituting Equations 12, 15, 16 into boundary condition (9), which specifies that the total concentration gradient vanishes at $\lambda = \delta$, one obtains

$$\begin{aligned} \delta = & \frac{N/r}{(1 + \beta_K \Omega e^\delta) \left[e^\delta (\delta - 1 - \beta_u \Omega) + \frac{\beta_u \Omega}{2} e^{2\delta} + 1 + \frac{\beta_u \Omega}{2} \right]}. \end{aligned} \quad (19)$$

Integration of Equation (19) gives

$$\begin{aligned} \delta_1 + N\xi/r = & \frac{\beta_u \beta_K \Omega^2}{6} e^{3\delta} + \left(\frac{\beta_u \Omega}{4} - \frac{3\beta_K \Omega}{4} - \frac{\beta_u \beta_K \Omega^2}{2} \right) e^{2\delta} + \\ & + \frac{\beta_K \Omega}{2} \delta e^{2\delta} + \left(\frac{\beta_u \beta_K \Omega^2}{2} + \beta_K \Omega - \beta_u \Omega - 2 \right) e^\delta + \\ & + \delta e^\delta + \left(1 + \frac{\beta_u \Omega}{2} \right) \delta. \end{aligned} \quad (20)$$

Using boundary condition (10),

$$\delta_1 = -2 + \frac{\beta_u \beta_K \Omega^2}{6} + \frac{\beta_K \Omega}{4} - \frac{3\beta_u \Omega}{4} \approx -2.$$

Equation (20) is implicit in δ , and may be solved for given r , ζ , N by Newton's Method of Successive Approximations (Abramowitz and Stegun, 1970).

Because of the large number of terms involved, the equations will now be simplified by writing $\beta_u = \beta_K = \beta$. Equations 13, 17, 18 become

$$\begin{aligned} \chi = \frac{r}{N} & [\beta\Omega(e^\delta - e^\lambda) + (\delta - \lambda)] + \\ & + \frac{\delta r(1 + \beta\Omega e^\delta)}{N^2} \left[\frac{\beta^2 \Omega^2}{6} (e^{3\lambda} - e^{3\delta}) - \right. \\ & - \left(\frac{\beta^2 \Omega^2}{2} + \frac{\beta\Omega}{2} \right) (e^{2\lambda} - e^{2\delta}) + \frac{\beta\Omega}{2} (\lambda e^{2\lambda} - \delta e^{2\delta}) + \\ & \left. + (\lambda e^\lambda - \delta e^\delta) + (\alpha_1 \beta\Omega - 2 - \beta\Omega) (e^\lambda - e^\delta) + \alpha_1 (\lambda - \delta) \right] \end{aligned} \quad (21)$$

where

$$\alpha_1 = 1 + \frac{\beta\Omega}{2} + (r-1) \left[e^\delta (\delta - 1 - \beta\Omega) + \frac{\beta\Omega}{2} e^{2\delta} + 1 + \frac{\beta\Omega}{2} \right]. \quad (22)$$

$$\dot{\delta} = \frac{N/r}{(1 + \beta\Omega e^\delta) \left[e^\delta (\delta - 1 - \beta\Omega) + \frac{\beta\Omega}{2} e^{2\delta} + 1 + \frac{\beta\Omega}{2} \right]} \quad (23)$$

and

$$\begin{aligned} N\zeta/r - 2 &= \frac{\beta^2 \Omega^2}{6} e^{3\delta} - \left(\frac{\beta^2 \Omega^2}{2} + \frac{\beta\Omega}{2} \right) e^{2\delta} + \\ &+ \frac{\beta\Omega}{2} \delta e^{2\delta} + \left(\frac{\beta^2 \Omega^2}{2} - 2 \right) e^\delta + \\ &+ \delta e^\delta + \left(1 + \frac{\beta\Omega}{2} \right) \delta. \end{aligned} \quad (24)$$

In neutral stratification $L = \infty$ so that $\Omega = 0$ and the solution becomes

$$\chi = \frac{r}{N} (\delta - \lambda) + \frac{\delta r}{N^2} [(\lambda e^\lambda - \delta e^\delta) - 2(e^\lambda - e^\delta) + \alpha_1 (\lambda - \delta)] \quad (21N)$$

where

$$\alpha_1 = 1 + (r - 1) [e^{\delta}(\delta - 1) + 1] \tag{22N}$$

$$\dot{\delta} = \frac{N/r}{e^{\delta}(\delta - 1) + 1} \tag{23N}$$

$$(\delta - 2)e^{\delta} + \delta = N\xi/r - 2. \tag{24N}$$

Although it is straightforward to determine r using boundary condition Equation (11), the integration involves many terms, particularly for $\Omega \neq 0$, and will not be performed here. For several values of Ω and ξ , the value of r which satisfies Equation (11) with $N = 0.25$ has been evaluated, and is plotted in Figure 1. These curves are negligibly altered by the alternative choice (corresponding to $K = K_m$) of $N = 0.16$.

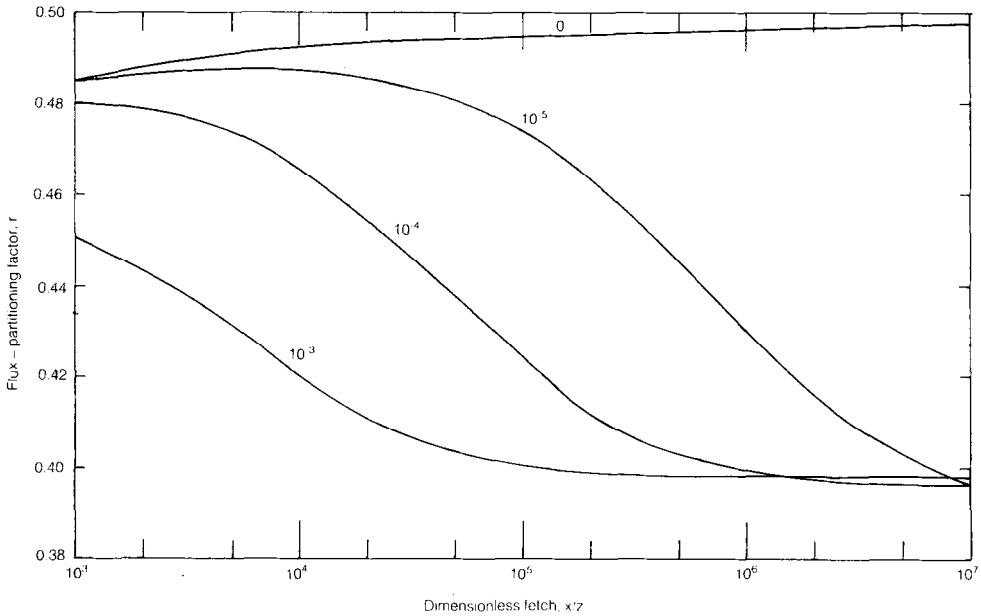


Fig. 1. Flux-partitioning factor r as a function of x/z_0 for several values of z_0/L .

In practise it was found that incorporation of the precise value of r which satisfies Equation (11) is disadvantageous – the total horizontal mass flux becomes correct at the expense of introducing a small error in ground-level concentration (as compared with the trajectory-simulation model described in Section 4). Rather than improving the prediction near $\lambda = \delta$, the optimisation with respect to r deteriorates the accuracy near ground, presumably because there are constraints on both χ and $\partial\chi/\partial\lambda$ at $\lambda = \delta$, but on $\partial\chi/\partial\lambda$ alone at $\lambda = 0$. It is therefore recommended that a value of 0.5 is used for r . All concentration profiles presented here use $r = 0.5$ unless otherwise noted.

Figure 2 shows the dimensionless concentration profiles a distance $\xi = 10^4$ downwind of the leading edge of an area source at ground. The contributions from χ_0 and χ_1 are

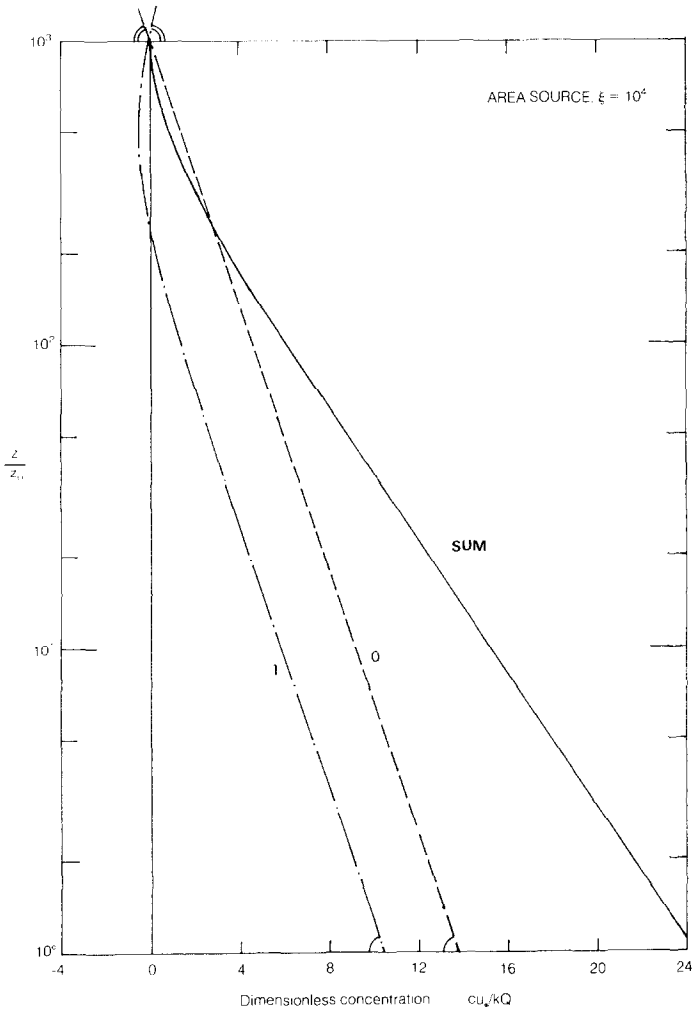


Fig. 2. The contributions χ_0 and χ_1 to the total dimensionless concentration χ at a distance $\xi = 10^4$ from the leading edge of an area source in the neutral surface layer.

separately shown, and it may be seen how the component profiles are consistent with the boundary conditions.

3. Ground-level Line Source

The concentration profile at x due to a line source of unit source strength at $x = 0$ may be obtained from the profile for an area source of unit strength extending from $x = 0$ to $x = x$ by writing

$$c' = \lim_{\Delta x \rightarrow 0} \frac{c''(x + \Delta x) - c''(x)}{\Delta x} = \frac{\partial c''}{\partial x}$$

from which it follows that

$$\chi' = \frac{z_0 c' u_*}{kQ} = \frac{\partial}{\partial \xi} \left(\frac{c'' u_*}{kQ} \right) = \frac{\partial \chi}{\partial \xi}$$

where $z_0 c' u_* / kQ$ is the dimensionless concentration due to a line source of strength Q [$\text{cm}^{-1} \text{s}^{-1}$] and (as before) $c'' u_* / kQ$ is the dimensionless concentration due to an area source of strength Q [$\text{cm}^{-2} \text{s}^{-1}$].

Therefore the solution for a line source may be obtained by differentiating Equation (21). Define

$$\begin{aligned} G(\lambda, \delta) = & \frac{\beta^2 \Omega^2}{6} (e^{3\lambda} - e^{3\delta}) - \left(\frac{\beta^2 \Omega^2}{2} + \frac{\beta \Omega}{2} \right) (e^{2\lambda} - e^{2\delta}) + \\ & + \frac{\beta \Omega}{2} (\lambda e^{2\lambda} - \delta e^{2\delta}) + (\lambda e^\lambda - \delta e^\delta) + \\ & + (\alpha_1 \beta \Omega - 2 - \beta \Omega) (e^\lambda - e^\delta) + \alpha_1 (\lambda - \delta). \end{aligned} \quad (25)$$

Then

$$\begin{aligned} \dot{G} = & -\dot{\delta} \left[\frac{\beta^2 \Omega^2}{2} e^{3\delta} - \left(\beta^2 \Omega^2 + \frac{\beta \Omega}{2} \right) e^{2\delta} + \beta \Omega \delta e^{2\delta} + \delta e^\delta + \right. \\ & \left. + (\alpha_1 \beta \Omega - 1 - \beta \Omega) e^\delta + \alpha_1 + \delta \dot{\alpha}_1 - (e^\lambda - e^\delta) \beta \Omega \dot{\alpha}_1 \right]. \end{aligned} \quad (26)$$

From (22),

$$\dot{\alpha}_1 = \dot{\delta} (r-1) [(\delta - \beta \Omega) e^\delta + \beta \Omega e^{2\delta}]. \quad (27)$$

From (23),

$$\ddot{\delta} = -\dot{\delta}^2 \left[\frac{(\delta - \beta \Omega) e^\delta + \beta \Omega e^{2\delta}}{e^\delta (\delta - 1 - \beta \Omega) + \frac{\beta \Omega}{2} e^{2\delta} + 1 + \frac{\beta \Omega}{2}} + \frac{\beta \Omega e^\delta}{1 + \beta \Omega e^\delta} \right]. \quad (28)$$

The line-source solution is obtained by substituting Equations (22–28) into the derivative of Equation (21),

$$\begin{aligned} \chi' = & \frac{r \dot{\delta}}{N} (1 + \beta \Omega e^\delta) + \frac{r}{N^2} [\dot{\delta} (1 + \beta \Omega e^\delta) \dot{G}] + \\ & + \frac{r \dot{G}}{N^2} [(1 + \beta \Omega e^\delta) \ddot{\delta} + \beta \Omega e^\delta \dot{\delta}^2]. \end{aligned} \quad (29)$$

Under neutral stratification, Equation (29) simplifies to

$$\chi' = \frac{r \ddot{\delta}}{N^2} [(\lambda e^\lambda - \delta e^\delta) - 2(e^\lambda - e^\delta) + (\lambda - \delta)] \quad (29N)$$

where

$$\ddot{\delta} = -r\delta\dot{\delta}^3 e^{\delta}/N \quad (28N)$$

and $\dot{\delta}$ and δ are obtained from Equations (23N, 24N).

By differentiating (29N) it may be shown that

$$\left(\frac{\partial\chi'}{\partial\lambda}\right)_{\lambda=0} = 0 \quad \left(\frac{\partial\chi'}{\partial\lambda}\right)_{\lambda=\delta} \neq 0.$$

The concentration gradient vanishes at ground, as required downwind of a line source emitting an admixture which is not absorbed by the ground. However the concentration gradient does not vanish at $\lambda = \delta$. It is not possible to obtain a line-source solution including only the first two terms ($\chi_0 + \chi_1$) which satisfies zero total concentration gradient at both $\lambda = 0$ and $\lambda = \delta$.

In order to determine r , the line source solution may be forced to obey

$$\int_0^{\delta} \chi'(\xi, \lambda) [\lambda + \beta_u \Omega (e^{\lambda} - 1)] e^{\lambda} d\lambda = 1. \quad (11L)$$

Because χ' is given by $\partial\chi/\partial\xi$, Equation (11L) is simply the derivative of Equation (11): that value of r which ensures that the plane-source solution satisfies Equation (11) also ensures that the line-source solution satisfies Equation (11L).

Equation (29) may also be interpreted as giving the cross-wind integrated (arc-integrated, equivalent two-dimensional) concentration at a distance (radius) ξ from a continuous ground-level point source if u is interpreted as the cup windspeed. In Section 5.2 solutions given by Equation (29) will be compared with measurements of dispersion from a ground-level point source.

4. Comparison of Analytical Solutions with Trajectory-simulation Model

Wilson *et al.* (1981a, b, c) have described a Lagrangian model of turbulent dispersion in inhomogeneous turbulence. Particle trajectories are numerically simulated by assuming that the important statistics of the fluctuating vertical velocity which must be incorporated are the standard deviation σ_w and the Lagrangian timescale $\tau_L(z)$ which is a measure of the temporal persistence of the Lagrangian vertical velocity. Horizontal motion occurs at a steady height-dependent velocity (no fluctuation in the horizontal windspeed). The trajectory-simulation (TS) model was shown to be in excellent agreement both with analytical solutions for homogeneous turbulence and turbulence with power-law wind and diffusivity profiles, and with observations of dispersion in the atmospheric surface layer. For further details the reader is referred to the reports above. The predictions of the TS model to be given here were obtained following the method of Wilson *et al.* (1981c). The vertical velocity record was obtained using a Markov chain, with $\sigma_w = 1.25u_*$ and $\Lambda_L = \sigma_w \tau_L = 0.5z/(1 + 5z/L)$. The horizontal velocity was

given by Equation (4) with $\beta_u = 5$. In the following comparisons the TS model should be regarded as the correct solution, and the approximate analytical solution as being satisfactory only to the extent that it agrees with the TS model.

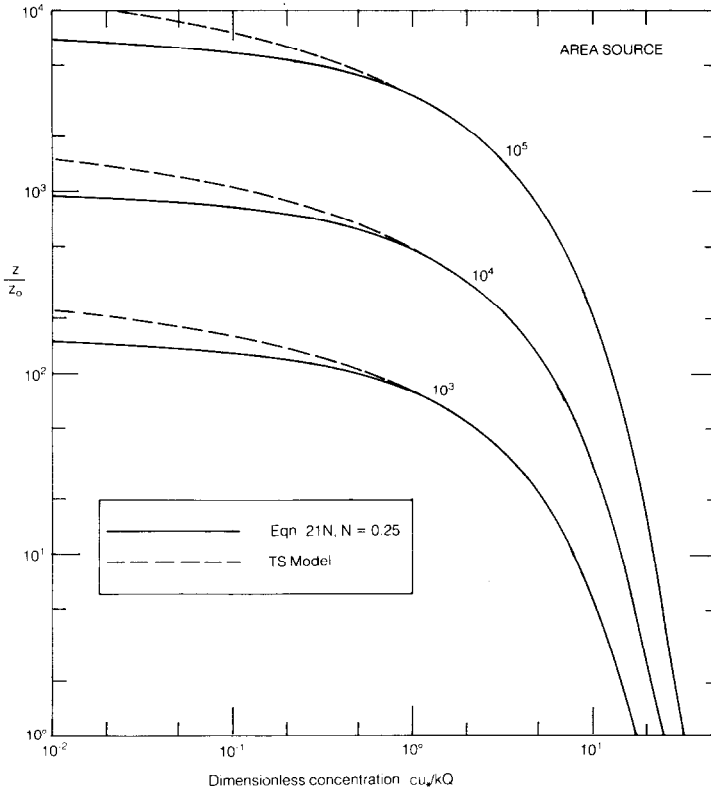


Fig. 3. Dimensionless concentration profiles at a distance $\xi = (10^3, 10^4, 10^5)$ from the leading edge of an area source in the neutral surface layer, according to the trajectory-simulation model and the approximate analytical solution to the diffusion equation.

Figure 3 compares the TS solution and the analytical solution for the dimensionless concentration profile at a distance $\xi = (10^3, 10^4, 10^5)$ downwind of the leading edge of a continuous area source at $z = z_0$ in the neutral surface layer. The two solutions are in very good agreement out to well above the height $\lambda_{1/10}$ where concentration falls to $1/10^{\text{th}}$ of the surface value. It appears from Figure 3 that the analytical solution does not conserve mass. The explanation is that there is a difference between the solutions at lower height which is so small as to disappear on a logarithmic concentration axis. Figure 4 shows the solutions for the concentration profile at $\xi = 10^4$ due to an area source at z_0 for values of z_0/L ranging from neutral to very stable stratification. On a linear concentration axis the small percentage differences between the TS model and the analytical solution at low levels are visible.

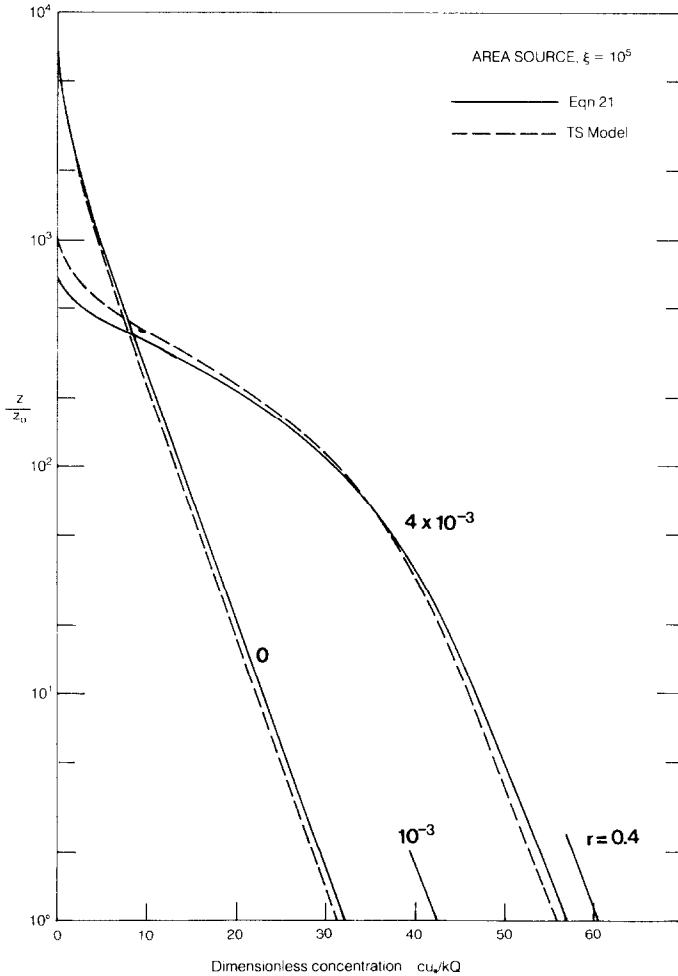


Fig. 4. Dimensionless concentration profiles at a distance $\xi = 10^5$ from the leading edge of an area source for z_0/L ($0, 10^{-3}, 4 \times 10^{-3}$).

Figure 5 compares the TS solution and the analytical solution for the concentration profile at a dimensionless distance $\xi = (10^3, 10^4, 10^5)$ downwind of a continuous line source at $z = z_0$ in the neutral surface layer. There is excellent agreement between the two solutions up to a dimensionless height of $z/z_0 \approx \xi/100$, so that for many purposes the analytical solutions should be adequate. Figure 6 shows the profiles at $\xi = 10^5$ for a line source at z_0 with several values of z_0/L . Again there is good agreement with the TS model at heights well below δ . For $z_0/L = 4 \times 10^{-3}$, the ground-level concentration according to the analytical solution with $r = 0.4$ is also plotted, to demonstrate the adverse effect of forcing the analytical solution to conserve mass.

The profile for $\xi = 10^3$ in Figure 5 may be compared with that obtained by Yamamoto and Shimanuki (1961) by numerical integration of the diffusion equation. Yamamoto and Shimanuki give a higher value of $z_0 c_w/kQ$ at ground (4.1×10^{-3} as opposed to 2.8×10^{-3} for the present estimate) in consequence of having set the mass diffusivity

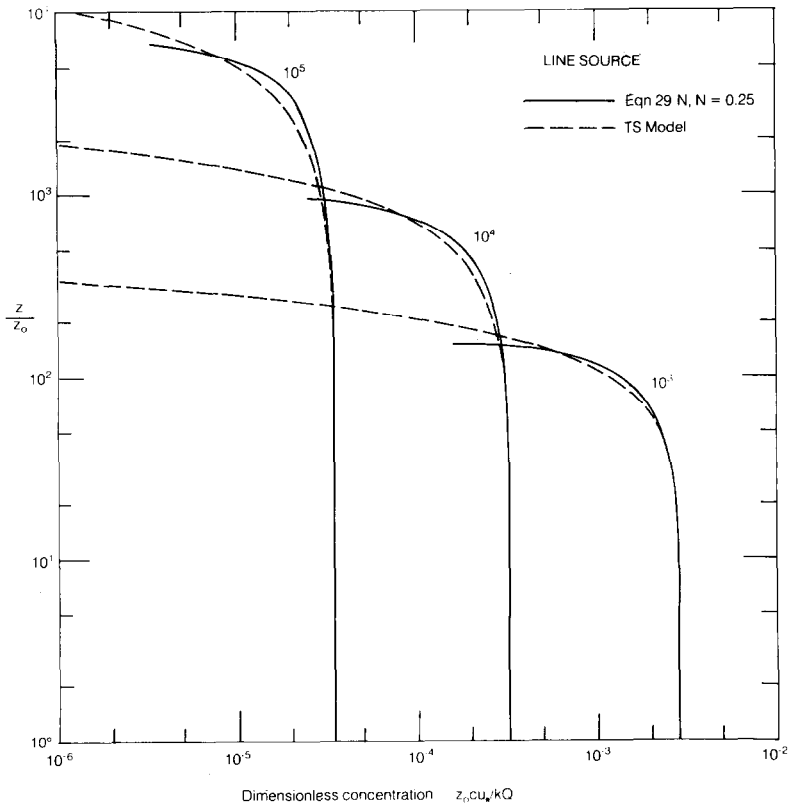


Fig. 5. Dimensionless concentration profiles at a distance $\xi = (10^3, 10^4, 10^5)$ downwind of a line source in the neutral surface layer.

equal to the eddy viscosity. At a longer fetch, $\xi = 5 \times 10^3$, the solutions given by the numerical integration and the analytical solution are respectively 10^{-3} and 6.0×10^{-4} .

5. Comparison of Analytical Solutions with Experimental Data

5.1. AREA SOURCE

Consider a disc of radius R over which the source strength is constant, and a tower at the axis of the disc. Assuming that there is no correlation between the instantaneous wind direction and the field of total horizontal and vertical velocity, and that the temporal and spatial persistence of the wind field is sufficient to ensure that trajectories across the disc exhibit little lateral meandering, dispersion from the source may be regarded as a two-dimensional process with horizontal speed $\sqrt{u^2 + v^2}$. Therefore the analytical solution for the concentration profile at the downwind edge of an area source of length R may be applied to this situation, if u is interpreted as the cup windspeed.

Denmead (personal communication) has performed experiments to determine the rate of loss of nitrogen as ammonia gas (NH_3) to the atmosphere from a small fertilised plot

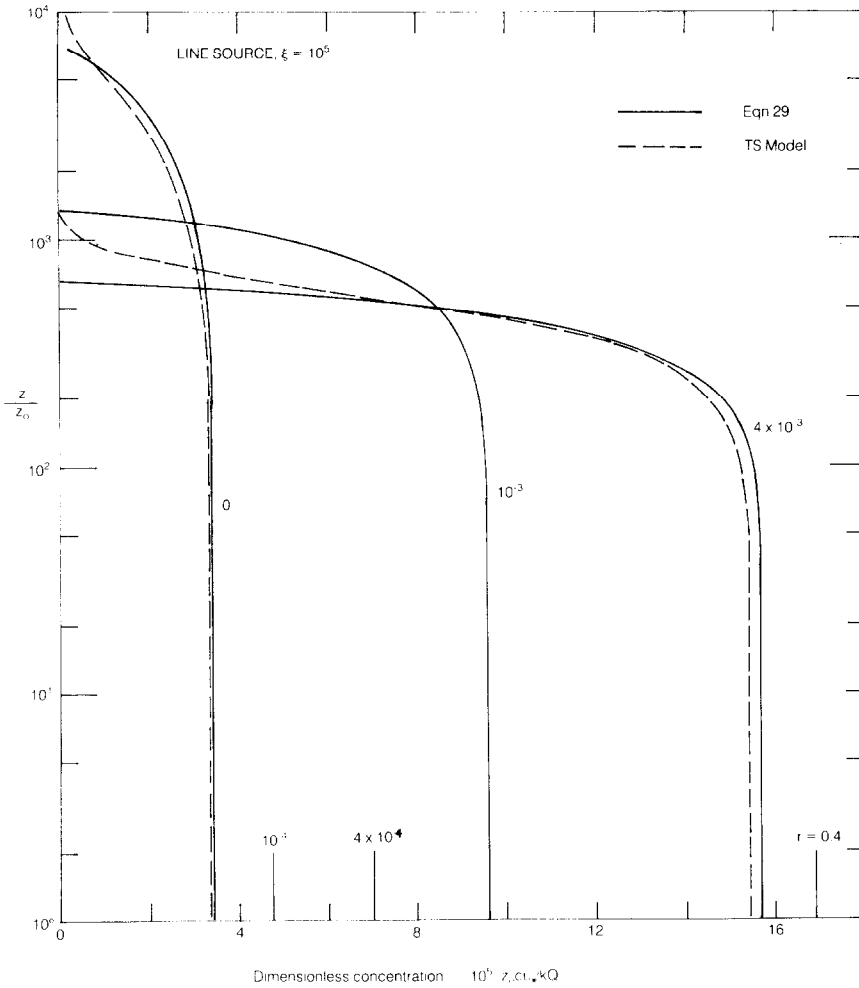


Fig. 6. Dimensionless concentration profiles at a distance $\xi = 10^5$ downwind of a line source for $z_0/L = (0, 10^{-3}, 4 \times 10^{-3})$.

of pasture with circular boundary. Observations for an experiment with $R = 25$ m, $z_0 = 2.32$ cm, $d = 15$ cm (displacement height) and $u_* = 14.5$ cm s^{-1} are compared in Figure 7 with the analytical solutions with $N = 0.25$ and $N = 0.16$. Note that the source strength, which is required in order to form the observed dimensionless concentration, was obtained by integrating the observed profile of \bar{uc} from $z = z_0$ to $z = \infty$, for this experiment having the value $Q = 13.9 \mu g m^{-2} s^{-1}$. The solution with $N = 0.25$ is certainly a better fit to the data than $N = 0.16$ (corresponding to $K = K_m$). If the discrepancy at the lowest level is real, it indicates that the source strength was probably decreasing towards the centre of the plot, a possibility which can not be accounted for in the analytical solution.

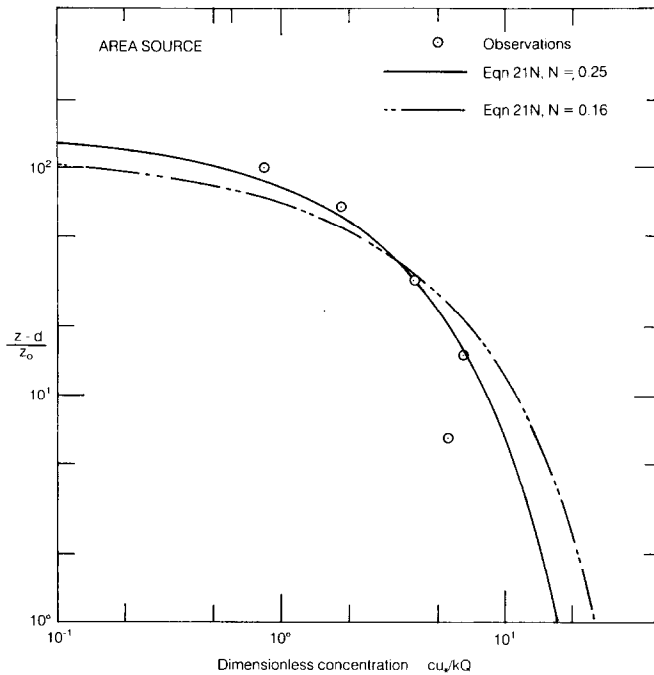


Fig. 7. Comparison of the observed profile of dimensionless concentration at the centre of a source disc of dimensionless radius $\xi = 1.08 \times 10^3$ with the approximate analytical solution to the diffusion equation.

5.2. LINE SOURCE

The Project Prairie Grass (PPG) experiments are described in reports by Barad (1958) and Haugen (1959). The time-averaged concentration at $z = 150$ cm downwind of a continuous point source of sulphur dioxide (SO_2) was measured along arcs of radius 50, 100, 200, 400, and 800 m. The vertical concentration profile was measured at the 100 m arc. For comparison with a two-dimensional model, equivalent two-dimensional concentrations may be obtained by integrating the concentration around each arc, and the vertical profile of crosswind-integrated concentration at $x = 100$ m may be obtained by using the profile shape observed to scale the value of cross-wind integrated concentration at $z = 150$ cm.

Run 33 was performed in near neutral stratification. Figure 8 compares the observations with the prediction of the TS model and the analytical solution, Equation (29N). The TS model prediction (obtained using $\sigma_w = 1.25u_*$, $\Lambda_L = 0.5z$, $u = (u_*/0.4) \ln(z/z_0)$)[†] agrees very closely with the observations at all levels, and is therefore superior to the analytical solution. However the TS solution used 2000 s of computer time, the analytical solution much less than 1 s. With $N = 0.25$ the prediction of the analytical solution for the near-ground concentration is satisfactory.

[†] And $z_0 = 0.75$ cm, which with $u_* = 59$ cm s⁻¹ gives a good fit to the observed wind profile.

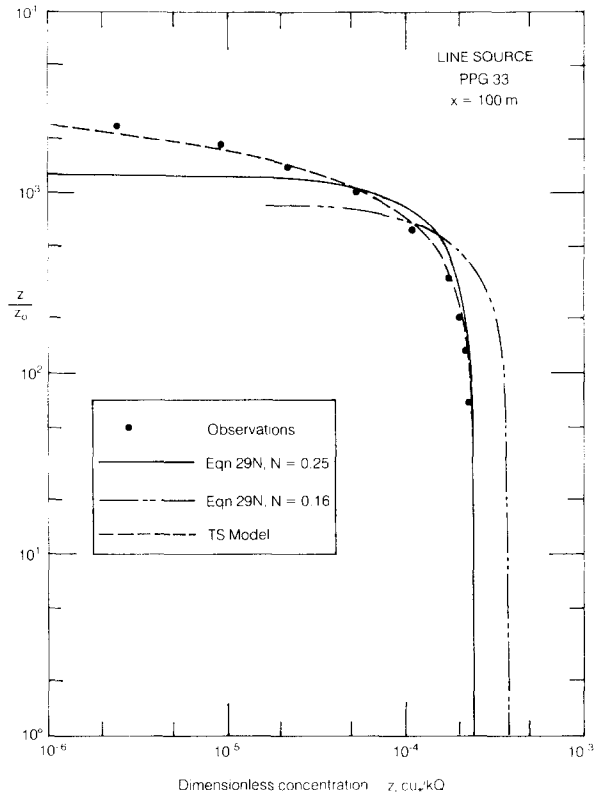


Fig. 8. Comparison of the observations of Project Prairie Grass run 33 (near neutral stratification) with the trajectory-simulation model and with the approximate solution to the diffusion equation.

TABLE I

Values of L and u_* derived for the Project Prairie Grass runs (1.0, -2 implies 1.0×10^{-2})

Run	$\Delta T/\Delta u$ ($^{\circ}\text{K s cm}^{-1}$)	L (m)	u_* (cm s^{-1})	Run	$\Delta T/\Delta u$ ($^{\circ}\text{K s cm}^{-1}$)	L (m)	u_* (cm s^{-1})
17 -	2.2, -3	77	22	37	1.8, -3	127	30
18	4.8, -3	31	20	38	1.4, -3	150	28
21	1.3, -3	240	40	41	3.2, -3	54	23
22	1.1, -3	330	49	42	2.0, -3	152	41
23	1.3, -3	240	42	46	1.9, -3	160	39
24	7.4, -4	420	41	53	1.5, -2	5.1	10.1
28	4.0, -3	31	17	54	4.4, -3	45	27
29	4.5, -3	43	26	55	1.7, -3	170	40
32	1.1, -2	8.1	11.5	56	2.5, -3	94	32
35	1.5, -2	3.5	6.8	58	1.1, -2	7.2	10.8
35s	2.6, -3	72	25	59	8.3, -3	12.9	14.1
36	6.6, -3	11.4	9.9	60	3.3, -3	73	32

As a comprehensive test of the ability of the analytical solution to predict near-ground concentration, values of z_0cu_x/kQ (dimensionless crosswind-integrated concentration) have been calculated for each arc of each of the stable Project Prairie Grass runs summarised in Table I. In order to determine u_* and L , for each run a graph of observed $u(z)$ versus observed temperature $T(z)$ was plotted to obtain an estimate of the slope $\Delta T/\Delta u$, which should be independent of height, and is related to u_*/L by

$$\frac{\Delta T}{\Delta u} = \frac{\bar{T}}{kg} \frac{u_*}{L}$$

This relationship follows from the recommendation of Dyer (1974) that in stable stratification $\phi_m = \phi_H$ (where ϕ_H is the Monin-Obukhov function for heat). The value of u_*/L thus obtained was substituted into the linear term of the log/linear wind profile, Equation (4)

$$u(z) = \frac{u_*}{k} \ln \frac{z}{z_0} + \frac{5(z - z_0)}{k} \frac{u_*}{L}$$

with $k = 0.4$ and $z_0 = 0.6$. The value of u_* was then determined from this equation by substituting the observed windspeed at the lowest height where $u > 80 \text{ cm s}^{-1}$.

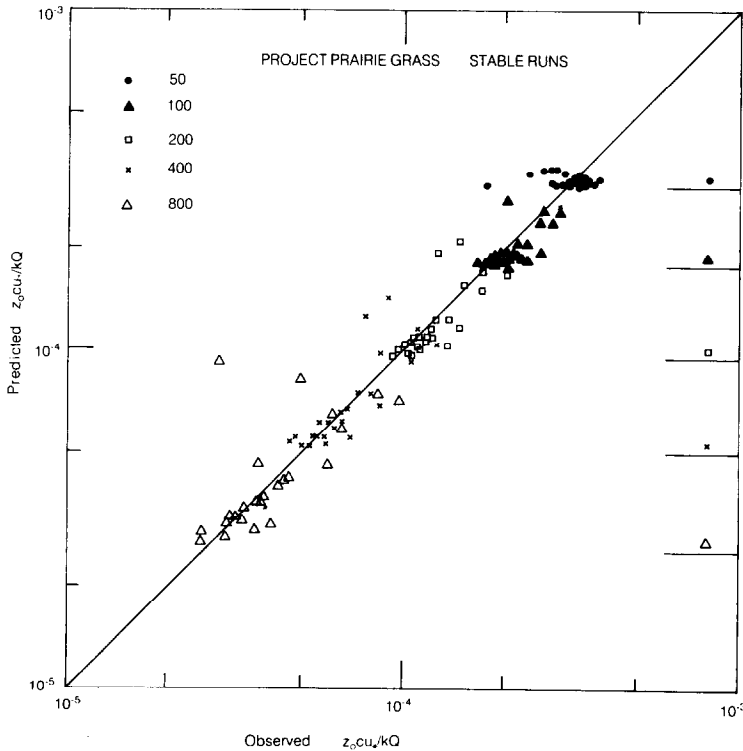


Fig. 9. Observed and predicted values of the dimensionless crosswind-integrated concentration at $z = 150 \text{ cm}$ and $x = (50, 100, 200, 400, 800 \text{ m})$ for Project Prairie Grass runs occurring in stable stratification.

In Figure 9 the observed values of crosswind-integrated concentration are compared with predictions obtained using $N = 0.25$. The agreement is reasonably good. On the right-hand side of the graph, the horizontal lines give the analytical solution without any stability correction (Equation (29N)). The effect of the stability correction is to move the plotted points upward to higher values of predicted concentration, and it appears that the stability correction is satisfactory.

Table II gives the average values of the ratio of observed to predicted concentration at each of the 5 downwind distances, for $N = 0.25$ and $N = 0.16$. The improvement resulting from using $K = 1.56K_m$ rather than $K = K_m$ is large.

TABLE II
Average ratios of observed/predicted concentration

	$N = 0.25 (K = 1.56K_m)$					$N = 0.16 (K = K_m)$				
Fetch (<i>m</i>)	50	100	200	400	800	50	100	200	400	800
Average $\frac{\text{observed}}{\text{predicted}}$	0.98	1.05	1.04	0.99	1.02	0.84	0.78	0.74	0.70	0.73
Sample standard deviation	0.16	0.14	0.15	0.15	0.23	0.13	0.10	0.10	0.11	0.16

Nieuwstadt and van Ulden (1978) compared numerical solutions with the PPG data, for two choices of the (stable) eddy diffusivity,

$$(a) \quad K = 0.47u_*z/(1 + 6.4(z/L))$$

$$(b) \quad K = 0.47u_*z/(1 + 4.7(z/L)).$$

They concluded that in stable conditions there was 'comparable agreement between calculated results and measurements for both alternatives'. This is not surprising in view of the close similarity between the two K -profiles. Nieuwstadt and van Ulden used $k = 0.35$, so that the value of N corresponding to their formulations for K is $N = 0.47 \times 0.35 = 0.16$. According to Table I this is not the best choice.

6. Conclusion

The near-ground concentration profile due to a ground-level area or line source in the stable or neutral surface layer is adequately described by a simple approximate solution to the diffusion equation. The close agreement between the analytical (Eulerian) solution and the trajectory-simulation (Lagrangian) solution confirms the validity of the relationship $K = \sigma_w \Lambda_L$ (where Λ_L is the Lagrangian length scale) for a ground-level source in inhomogeneous turbulence. Best agreement with observations is obtained using $\Lambda_L = 0.5z/(1 + 5z/L)$ which implies $K = 0.63u_*z/(1 + 5z/L)$, or $K = 1.56K_m$ where $K_m = 0.4u_*z/(1 + 5z/L)$ is the eddy viscosity.

To date, an effort to obtain an analogous solution for the case of unstable stratification has been unsuccessful.

Acknowledgements

This work was carried out while the author was a post-doctoral fellow at Atmospheric Environment Service, Downsview, Ontario, under the support of the National Sciences and Engineering Research Council of Canada. The author is grateful to Dr O. T. Denmead for supplying experimental data, and to Dr C. S. Matthias for helpful comments.

References

- Abramowitz, M. and Stegun, I. A.: 1970, *Handbook of Mathematical Functions*, Dover Publications Inc., New York.
- Barad, M. L.: 1958, 'Project Prairie Grass, a Field Program in Diffusion (Vol. II)', Geophysical Research Papers No. 59, Air Force Cambridge Research Centre – TR-58-235(II).
- Dyer, A. J.: 1974, 'A Review of Flux-profile Relationships', *Boundary-Layer Meteorol.* **7**, 363–372.
- Haugen, D. A.: 1959, 'Project Prairie Grass, a Field Program in Diffusion (Vol. III)', Geophysical Research Papers No. 59, Air Force Cambridge Research Centre – TR-58-235(III).
- Lebedeff, S. A. and Hameed, S.: 1976, 'Laws of Effluent Dispersion in the Steady-state Atmospheric Surface Layer in Stable and Unstable Conditions', *J. Appl. Meteorol.* **15**, 326–336.
- Nieuwstadt, F. T. M. and van Ulden, A. P.: 1978, 'A Numerical Study on the Vertical Dispersion of Passive Contaminants from a Continuous Source in the Atmospheric Surface Layer', *Atmos. Environ.* **12**, 2119–2124.
- Panchev, S., Donev, E., and Godev, N.: 1971, 'Wind Profile and Vertical Motions above an Abrupt Change in Surface Roughness', *Boundary-Layer Meteorol.* **2**, 52–63.
- Philip, J. R.: 1959, 'The Theory of Local Advection: I', *J. Meteorol.* **16**, 535–547.
- Shwetz, M. E.: 1949, 'On the Approximate Solution of some Boundary-Layer Problems', *Appl. Mathematics Mech.* **13(3)**, (Moscow).
- van Ulden, A. P.: 1978, 'Simple Estimates for Vertical Diffusion from Sources Near the Ground', *Atmos. Environ.* **12**, 2125–2129.
- Webb, E. K.: 1970, 'Profile Relationships: The Log-linear Range, and Extension to Strong Stability', *Quart. J. Roy. Meteorol. Soc.* **96**, 67–90.
- Wilson, J. D., Thurtell, G. W., and Kidd, G. E.: 1981a, 'Numerical Simulation of Particle Trajectories in Inhomogeneous Turbulence, I: Systems with Constant Turbulent Velocity Scale', *Boundary-Layer Meteorol.* **21**, 295–313.
- Wilson, J. D., Thurtell, G. W., and Kidd, G. E.: 1981b, 'Numerical Simulation of Particle Trajectories in Inhomogeneous Turbulence, II: Systems with Variable Turbulent Velocity Scale', *Boundary-Layer Meteorol.* **21**, 423–441.
- Wilson, J. D., Thurtell, G. W., and Kidd, G. E.: 1981c, 'Numerical Simulation of Particle Trajectories in Inhomogeneous Turbulence, III: Comparison of Predictions with Experimental Data for the Atmospheric Surface Layer', *Boundary-Layer Meteorol.* **21**, 443–463.
- Yamamoto, G. and Shimanuki, A.: 1961, 'Numerical Solution of the Equation of Atmospheric Turbulent Diffusion (1)', *Sci. Reports Tohoku Univ.*, ser V, Geophysics **12**, 24–35.